Highly Efficient Blue Organic Light-Emitting Diodes Based on Intermolecular Triplet–Singlet Energy Transfer

ARTICLE *in* THE JOURNAL OF PHYSICAL CHEMISTRY C · SEPTEMBER 2013

Impact Factor: 4.77 · DOI: 10.1021/jp407397y

THE JOURNAL OF PHYSICAL CHEMISTRY C

Article

pubs.acs.org/JPCC

Highly Efficient Blue Organic Light-Emitting Diodes Based on Intermolecular Triplet−Singlet Energy Transfer

Dmytro Volyniuk,[†,‡] Vladyslav Cherpak,[‡] Pavlo Stakhira,[‡] Boris Minaev,[§] Gleb Baryshnikov,[§] Maryan Chapran,[‡] Ausra Tomkeviciene,[†] Jonas Keruckas,[†] and Juozas V. Grazulevicius*[,†]

[†]Department of Organic Technology, Kaunas University of Technology, Radvilenu pl. 19, LT-50254 Kaunas, Lithuania

[‡]Lviv Polytechnic National University, S. Bandera 12, 79013 Lviv, Ukraine

[§]Bohdan Khmelnytsky National University, Shevchenko 81, 18031 Cherkassy, Ukraine

Supporting Information

ABSTRACT: Diphenilamino-substituted carbazoles were used as guest compounds for the preparation of highly efficient blue organic light-emitting diodes based on the phenomenon of delayed fluorescence. It was shown that the spectra of the delayed fluorescence of host−guest systems are identical to those of the prompt fluorescence and in general coincide with the photoluminescence spectra of the guest films. The congruence of the prompt and delayed fluorescence spectra is explained by the effective intermolecular triplet−singlet (T → S) energy transfer from the excited T states of the host to the S states of the guest molecules. High external electroluminescence efficiency of the fabricated electroluminescent devices, reaching 17%, is comparable to that achieved in phosphorescence-based organic light-emitting diodes.

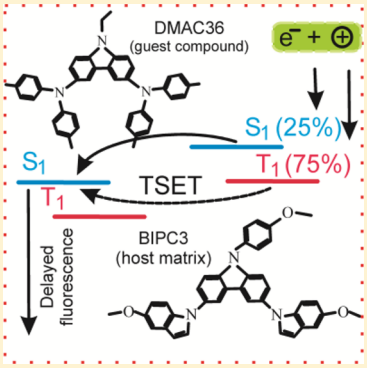

INTRODUCTION

The current level of development of organic light-emitting diodes (OLEDs) enables their effective application in low-cost flat panel display technology and in lighting.[1] Development of highly efficient blue OLEDs attracts special attention because their characteristics are thus far inferior to those of red or green devices.[2] This could be associated with the lower thermal and morphological stability of organic blue light-emitting materials, with the problems related to the synthesis of materials with good charge-transporting properties as well as with poor injection of charge carriers into organic blue emitting layers from the electrodes because of the large band gaps.[3] In recent years, much effort has been concentrated on the development of electrophosphorescent light-emitting devices based on the complexes of heavy transition-metals incorporating both singlet and triplet excitons because of high quantum efficiencies attained in such devices.[4] However, the high cost of heavy metal-based phosphorescent dyes is one of the key obstacles that hinders the widespread use of phosphorescent OLEDs.[4] Another approach in fabrication of efficient blue-emitting OLEDs is based on the use of the doped fluorescent host−emitter systems in simple device structures with balanced charge carrier transport.[5] Original possibility of fabrication of the highly efficient OLEDs employing the delayed fluorescence was recently demonstrated by Adachi et al.[6] In such OLEDs, the intramolecular spin up-conversion from nonradiative triplet state to the radiative singlet state is exploited. Both singlet and triplet excitons take part in generation of light emission in such devices without enhancement of spin−orbit coupling by heavy metal ions. However, the development of the corresponding host−guest systems is a complicated task because it is necessary to provide a proper energy matching of singlet and triplet levels for high exciton formation probability[6,7] and high thermal and morphological stability of the materials.[8]

The highly efficient violet-emitting compound 2,7-di[di(4-methylphenyl)amino]-9-ethylcarbazole (**DMAC27**) (fluorescence quantum yield of 0.46) and the blue-emitting 3,6-di[di(4-methylphenyl)amino]-9-ethylcarbazole (**DMAC36**) (Figure 1) were recently synthesized.[9] They display high thermal stability and form molecular glasses with glass transition temperatures of ca. 100 °C. However, the high lowest unoccupied molecular orbital (LUMO) level positions of these compounds, which are −1.75 eV (**DMAC27**) and −1.94 eV (**DMAC36**), make it difficult to provide directly an efficient injection of electrons from the cathode of thte OLED.

In this work we demonstrate highly efficient violet and blue OLEDs based on the triplet−singlet intermolecular energy transfer. Devices containing **DMAC27** or **DMAC36** as guest compounds incorporated into the 3,6-bis(5-methoxyindol-1-yl)-9-(4-methoxyphenyl)carbazole (**BIPC3**) host matrix were fabricated. **BIPC3** was earlier reported to be useful as a host material for phosphorescent OLEDs.[10] In addition, it is a blue-light-emitting material.[10] The mechanism of energy transfer which provides the delayed fluorescence in the fabricated host−

Received: July 25, 2013
Revised: September 24, 2013
Published: September 27, 2013

   dx.doi.org/10.1021/jp407397y | J. Phys. Chem. C 2013, 117, 22538−22544

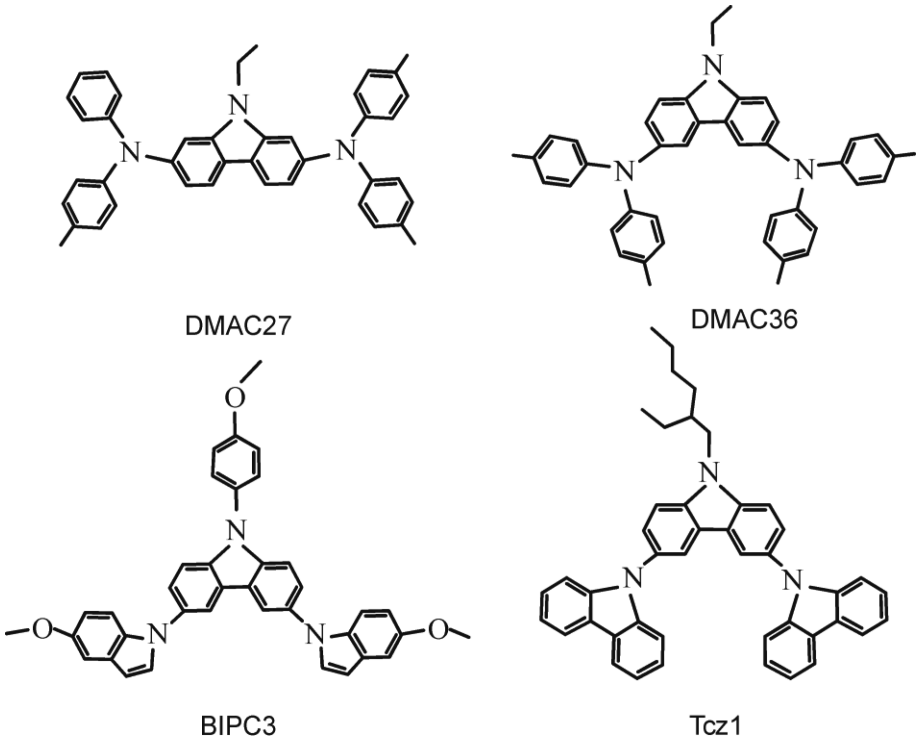

Figure 1. Chemical structures of **DMAC27**, **DMAC36**, **BIPC3**, and **TCz1**.

guest systems is theoretically substantiated by DFT calculations.

EXPERIMENTAL DETAILS

Device Fabrication. In the device fabrication, a CuI film was used as a hole-transporting material[11] and 3,6-di(9-carbazolyl)-9-(2-ethylhexyl)carbazole (**TCz1**) (Figure 1) was used as an electron-transporting material.[8,12,13] Devices A and B were fabricated by step-by-step vacuum deposition of different organic layers. The electroluminescent devices ITO/CuI (10 nm)/**BIPC3**:**DMAC27**(40 nm)/**TCz1** (7 nm)/Ca (7 nm)/Al (100 nm) (A) and ITO/CuI (10 nm)/**BIPC3**:**DMAC36** (40 nm)/**TCz1** (7 nm)/Ca (7 nm)/Al (100 nm) (B) were fabricated by successive deposition onto precleaned ITO coated glass substrate under vacuum of 10^{-5}Torr of the following layers: hole-injector CuI layer,[11] codeposited from one-source boat layer of **BIPC3** and **DMAC27** (**DMAC36**),[14] **TCz1** which served as electron-injection layer, and Ca/Al layer. The aluminum component of the cathode was used for passivation of the calcium electrode. This mode of construction permitted us to investigate the properties of the devices in ambient atmosphere at room temperature immediately after device fabrication. Additional passivation was not used.

TCz1 is a versatile compound previously shown to be useful as an effective electron-injection material,[13] which helps to provide a stepwise electron transfer from the Ca:Al cathode to the emissive layer. Its LUMO energy (−2.6 eV) is close to the cathode work function (−2.9 eV). **BIPC3** as a host is characterized by a higher LUMO energy (−1.3 eV); thus, a **TCz1** layer works as an intermediate electron-transfer layer between the cathode and the host matrix.

The thicknesses of the layers were measured by a NanoCalc 2000 reflectometry system. The active area of the obtained devices (A and B) was 3 × 2 mm^2.

For the measurements of photoluminescence and absorption spectra of the organic films, they were vacuum-deposited on quartz substrates. UV spectra were recorded with Cary 5000 UV−vis−NIR and Specord UV−vis spectrometers. The spectra of the prompt and delayed luminescence were recorded at room temperature using an LS55 fluorescence spectrometer and FL WinLab software. To separate the prompt and delayed luminescence spectra of the films of the molecular mixtures **DMAC27**:**BIPC3** and **DMAC36**:**BIPC3**, the emission was measured twice: immediately after excitation and with a delay after the pulse was turned off (the delay time was set to be ca. 30 μs).

The current density−voltage (*J*-*V*) characteristics were measured using a programmable test power LED300E (accuracy ±0.1%), and the electroluminescence (EL) spectra were recorded using the Ocean Optic USB2000 spectrometer. The brightness measurements were done using a calibrated photodiode.[15] Calibration of the photodetector was carried out using an RTN 20 radiometer (accuracy ±2%). The relative error of irradiance measurements was up to ±2%. External quantum efficiency (EQE) was estimated by the earlier reported procedure.[16]

Computational Details. The ground singlet-state geometry optimization of the compounds **DMAC27**, **DMAC36**, and **BIPC3** was performed by the DFT B3LYP/6-31G+(d)[17−19] level using the GAUSSIAN 09[20] package. Optimization of the triplet excited-state geometries of the studied compounds was performed by the same method at the framework of the unrestricted Kohn−Sham formalism. The IR and Raman spectra of the ground singlet and excited triplet states of the studied molecules were also calculated. All the calculated vibrational frequencies are real, which indicates the true minimum of the total energy on the potential energy hypersurface.

dx.doi.org/10.1021/jp407397y | J. Phys. Chem. C 2013, 117, 22538−22544

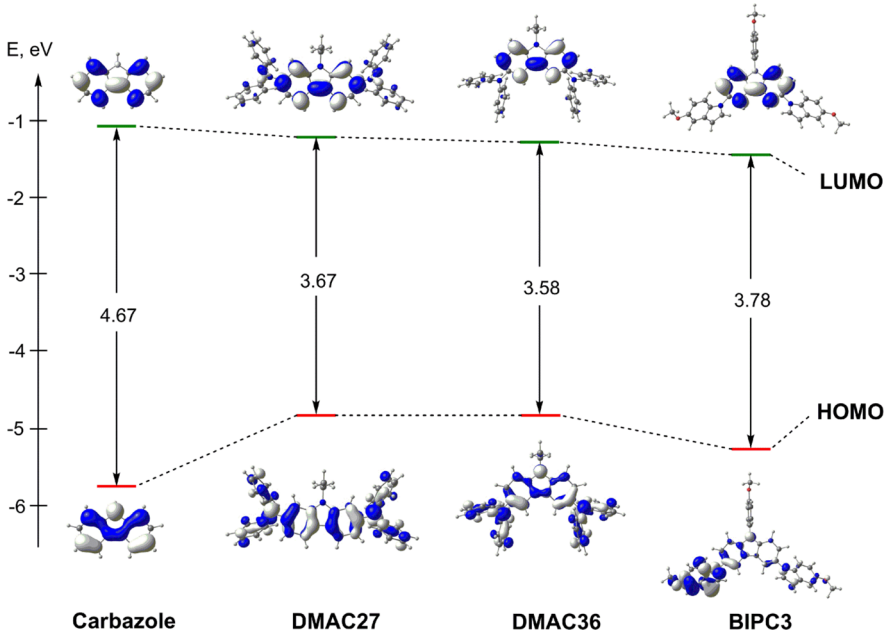

Figure 2. Energy diagram of the frontier molecular orbitals of carbazole, **DMAC27**, **DMAC36**, and **BIPC3**.

The electronic absorption spectra and triplet excited-state energies of the studied compounds were calculated by the time-dependent (TD) DFT method[21] using the same B3LYP/6-31+G(d) approach with the polarized continuum model (PCM)[22] incorporating the tetrahydrofuran (THF) species (ε = 7.43) as a model solvent. The same THF was also used as a solvent for the experimental measurements of the UV−vis spectra of **DMAC27**, **DMAC36** and **BIPC3**. The fitting of the electronic absorption spectra curves of the studied molecules was performed using the Gauss distribution function and a half-width of 3500 cm^{-1} with the SWizard 4.6 program package.[23]

RESULTS AND DISCUSSION

Geometries and Frontier Orbitals. The DTF-optimized geometries of **DMAC27**, **DMAC36**, and **BIPC3** are presented in Figure 2 with the shape of the frontier molecular orbitals of these compounds. The optimized conformations of the T_1 state are quite similar to the S_0 state geometries. The spin density in the T_1 state is mainly delocalized on the carbazole moiety (≈1.6) with equivalent contributions (at about 0.2) on each diphenylamine/indole branch. From the TD DFT/UB3LYP calculations, it is obvious that the T_1 state corresponds to the quasi-$\pi\pi^*$ type HOMO → LUMO excitation (Figure 2). The diphenylamine and indole substituents are not coplanar with the carbazole moiety, and highest occupied molecular orbital (HOMO) wave functions are partly delocalized across the whole species. For the guest emitters (**DMAC27** and **DMAC36**), all frontier molecular orbitals are concentrated on the carbazole nucleus, whereas in the **BIPC3** molecule the HOMO is more localized on an indole moiety. The symmetry of LUMO wave functions of **DMAC27**, **DMAC36**, and **BIPC3** corresponds mainly to the π-orbital of the carbazole nucleus. Thus, the T_1 excited state has a quasi-$\pi\pi^*$ orbital nature of the charge-transfer type. The low intensity of $S_0 \rightarrow S_1$ transition for **BIPC3** is caused by rotation (~55°) of the indole moiety relative to the carbazole fragment. Thus, the charge transfer upon the excitation is provided by the hyperconjugation effect between the indole and carbazole moieties which stipulates the relatively low intensity of $S_0 \rightarrow S_1$ transition.

The energies of the HOMO orbitals are in excellent agreement with those established by experimental electrochemical measurements,[9] while the calculated LUMO level energy is overestimated by ca. 0.6 eV (Table 1). The HOMO−LUMO energy gaps are equal to 3.67, 3.58, and 3.78 eV for **DMAC27**, **DMAC36**, and **BIPC3**, respectively, which qualitatively correlate with the optical band gaps of 3.06, 2.89, and 3.1 eV, respectively, estimated from the edges of the electronic absorption spectra.[9]

Table 1. Energies of Frontier Molecular Orbitals for the Studied Compounds, Calculated by DFT B3LYP/6-31G+(d) Method and Measured by Electrochemical Redox Potentials[a]

compound	*E* (HOMO) (eV)	*E* (LUMO) (eV)
DMAC27	−4.88 (−4.81)	−1.21 (−1.75)
DMAC36	−4.88 (−4.83)	−1.30 (−1.94)
BIPC3	−5.22	−1.44
TCz1	−5.8	−2.6

[a]Experimental values[9,10,12] are presented in parentheses.

The HOMO orbitals of **DMAC27** and **DMAC36** (Figure 2) are delocalized over the entire molecules with the primary contribution on the nitrogen atoms of the diphenylamino group. The HOMO orbital of **BIPC3** is quasidegenerate with HOMO-1, and both orbitals are predominantly localized on each indole moieties. One can note that HOMOs of **DMAC27** and **DMAC36** represent the mixtures of individual carbazole and diphenylamine orbitals. The 3,6-substituted carbazole derivative **DMAC36** has a big contribution from the *l* (π-type) lone pair on a nitrogen atom of the carbazole moiety. This contribution is absent in the 2,7-substituted derivative **DMAC27** because of the antisymmetric character of the carbazole counterpart of the HOMO wave function.

The LUMO orbitals (Figure 2) of the studied molecules are quite similar to each other and to the LUMO of the

dx.doi.org/10.1021/jp407397y | J. Phys. Chem. C 2013, 117, 22538−22544

Table 2. Calculated Parameters and Orbital Assignment of the $S_0 \rightarrow T_1$ and $S_0 \rightarrow S_1$ Transitions for Molecules of DMAC27, DMAC36, and BIPC3[a]

compound	excited state	λ (nm)	E (eV)	f	assignment
DMAC27	T_1	484	2.56	0.000	HOMO → LUMO 86%
	S_1	396 (384)	3.13	0.903	HOMO → LUMO 97%
DMAC36	T_1	466	2.66	0.000	HOMO → LUMO 90%
	S_1	407 (405)	3.05	0.018	HOMO → LUMO 97%
BIPC3	T_1	415	2.99	0.000	HOMO → LUMO 72%
	S_1	363 (360)	3.42	0.014	HOMO → LUMO 97%

[a]Experimental data[9] are in parentheses.

unsubstituted carbazole molecule. The energy of the LUMO level decreases monotonously in the series carbazole > **DMAC27** > **DMAC36** > **BIPC3**. In contrast, the HOMO energy levels of the diphenilamino-substituted species are strongly increased as compared with that of unsubstituted carbazole molecule (Figure 2).

The analysis of frontier molecular orbitals provides some information on the fluorescence efficiency of the studied active compounds. The first singlet−singlet electronic transition to the fluorescent S_1 excited state is assigned to the HOMO−LUMO single electron excitation for each of the studied molecules (Table 2). This transition corresponds to the charge transfer from the diphenylamine/indole fragments to the carbazole moiety with a large contribution from the local excitation in the later moiety (Figure 2). For the 2,7-substituted compound **DMAC27**, the $S_0 \rightarrow S_1$* electronic transition (violet) is fifty times more intense than the corresponding (blue) transition for the 3,6-substituted compound **DMAC36** (Table 2). This observation can be explained by the fact that the $S_0 \rightarrow S_1$* transition for the **DMAC27** compound mainly corresponds to the $\pi \rightarrow \pi^*$ excitation type, whereas the same transition for **DMAC36** can be assigned mostly to the low-intensity $l \rightarrow \pi^*$ excitation. The additional contribution to the $S_0 \rightarrow S_1$* transition intensity for compound **DMAC27** is caused by the common nonzero overlapping area of HOMO and LUMO orbitals on the diphenylamino groups (in contrast to **DMAC36** and **BIPC3**, Figure 2). Thus, the fluorescence quantum yield for the solution of **DMAC27** (Φ = 0.45, τ_{fl} = 1.4 ns) is much higher and the lifetime is lower in comparison with those of **DMAC36** (Φ = 0.11, τ_{fl} = 7 ns).[9] In the solid state, the more symmetrical molecular geometry of the 2,7-substituted carbazole derivative (similar to the C_s symmetry point group) favors closer molecular packing in the thin films, thereby facilitating an exciton migration. Such migration induces an exciton quenching, which results in the significantly reduced excited-state decay times (down to subnanoseconds) and fluorescence quantum yields (down to 0.04). Thus, in the solid phase, the singlet S_1 states of **DMAC27** are quenched, in contrast to those observed for the solutions, where the intrinsic molecular radiative properties dominate (Table 2).

The experimental and TD DFT-calculated absorption spectra (using the Gauss band form distribution) of the studied compounds are presented in Figure 3 with the theoretical oscillator strength for vertical transitions. The shapes of the experimental and theoretical spectral curves are similar; one can see the red-shifted deviations of the calculated spectra relatively to the experimental spectra. Our TD DFT calculations also slightly overestimate the absorption band intensity. In the electronic absorption spectrum of **DMAC27**, the $S_0 \rightarrow S_1$ transition corresponds to the first intense absorption band (Figure 3A and Table 2).

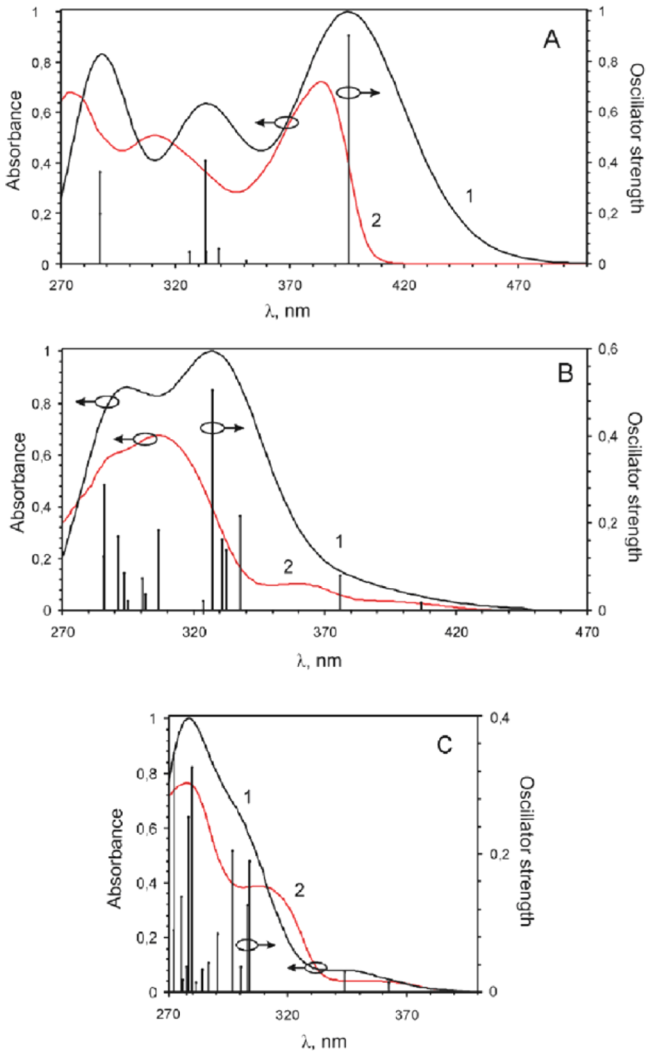

Figure 3. Calculated (1) and experimental (2) absorption spectra of **DMAC27** (A), **DMAC36** (B), and **BIPC3** (C).

In the UV−vis spectra of **DMAC36** and **BIPC3**, the $S_0 \rightarrow S_1$ transition corresponds to the weak broad shoulder in the regions of 380−420 nm and 340−390 nm, respectively. This shoulder also includes the weak $S_0 \rightarrow S_2$ absorption at 376 and 344 nm, respectively (Figure 3B,C). This is clearly seen in Figure 3B for the spectrum of **DMAC36**. More intense $S_0 \rightarrow S_n$ transitions (n = 3−6) in **DMAC36** produce the most strong absorption bands in the UV region. All the UV bands of the spectra shown in Figure 3 can be reasonably interpreted by TD DFT calculations.

The standard chosen half-width of 3500 cm^{-1} in the theoretical simulation of the absorption bands with the

dx.doi.org/10.1021/jp407397y | J. Phys. Chem. C 2013, 117, 22538−22544

Gaussian forms definitely overestimates the observed bandwidth (Figure 3) but does not hamper the qualitative assignment of all prominent features of the experimental spectra.

Optical and Photophysical Properties of the Vacuum-Deposited Films. Figure 4 presents the absorption and

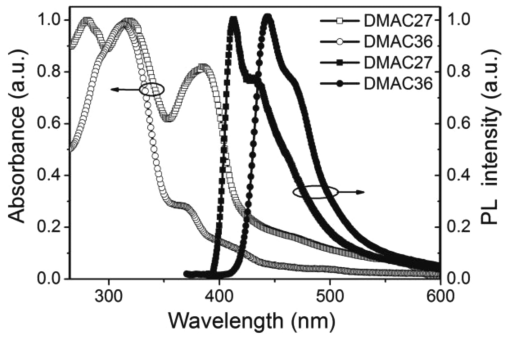

Figure 4. Normalized absorption and fluorescence spectra of the films of **DMAC27** and **DMAC36** prepared by vacuum deposition.

fluorescence spectra of the vacuum-deposited films of **DMAC27** and **DMAC36** recorded at room temperature. The shapes of the absorption and fluorescence bands of the films of these compounds are similar to those observed for the solutions.[9]

To confirm the presence of the energy transfer in the host–guest systems, we performed a study of photoluminescence spectra resolved into the prompt and delayed components (Figure 5). The spectra of the delayed fluorescence are identical to those of the prompt fluorescence of the guest–host systems and in general coincide with the photoluminescence spectra of the films of **DMAC27** and **DMAC36**. In the short-wavelength

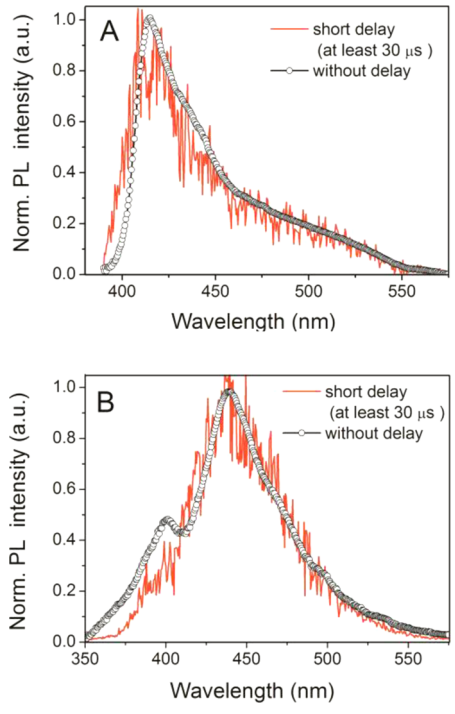

Figure 5. Normalized prompt and delayed fluorescence spectra of the films of the molecular mixtures **DMAC27:BIPC3** (A) and **DMAC36:BIPC3** (B) prepared by vacuum deposition.

region of the spectrum of the molecular mixture **DMAC36:-BIPC3** the fluorescence band of the **BIPC3** appears.[10] The congruence between the prompt and delayed fluorescence spectra of the molecular mixtures can be explained by the effective energy transfer from the excited states of the **BIPC3** matrix to the molecules of guests (**DMAC27** or **DMAC36**). To prove the efficiency of such mechanism on the electronic TD DFT backgrounds, we have recalculated the host–guest complex (**BIPC3** and **DMAC36**) accounting for spin–orbit coupling perturbation (Figure SM1 of the Supporting Information).

Figure 6 shows the spectra of electroluminescence of the devices. The shapes of the spectra of electroluminescence of

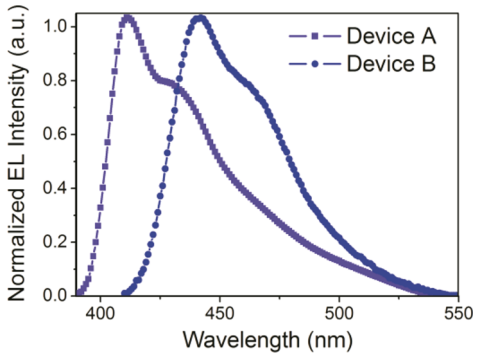

Figure 6. Electroluminescence spectra of device A and B recorded under the supplied voltage of 6 V.

device A and B are similar to those of photoluminescence spectra of the solid films of **DMAC27** and **DMAC36**, respectively. This observation confirms an efficient energy transfer from the host to the guest under the electrical biasing of the devices. **TCz1** was used as an electron-transporting material in the fabricated devices. In this way the **TCz1** layer is practically not populated by the excitons and can not provide any appreciable emission. We have also fabricated the devices without a **TCz1** layer, and their electroluminescence spectra are similar to those of the spectra of device A and B.

We assume that the electron–hole recombination starts in the volume of the **BIPC3** matrix which provides S_1 and T_1 excited states in these species under application of the external electric field (Figure 7).

The transition $T_1 \rightarrow S_0$ in **BIPC3** is spin forbidden and the transition $S_1 \rightarrow S_0$ is only slightly allowed, as follows from the calculated transition moment (Table 2) and from the discussed orbital features (Figure 2). Thus, we expect an effective $S_1 \rightarrow S_1$ intermolecular energy transfer from **BIPC3** to the guest emitters **DMAC27** and **DMAC36**, which explains prompt luminescence. By statistics, the S and T states are produced from the electron–hole recombination in a 1:3 ratio; thus, a huge concentration of the triplet states is formed in the host upon bias. As can be seen from Figure 7, the S_1 states of **DMAC27** and **DMAC36** are almost degenerate with the T_1 level of **BIPC3**. We suppose that the effective $T_1 \rightarrow S_1$ energy transfer (TSET) from **BIPC3** to **DMAC27** and **DMAC36** occurs. The T–S energy transfer in solid matrices is well-known,[24−26] and its characteristic features are completely applicable to our binary systems of **BIPC3** and guest molecules (**DMAC27**, **DMAC36**). The T–S energy transfer in solid solvents was predicted by Förster in 1959[25] and observed experimentally by Ermolaev and Sveshnikova in organic glasses

dx.doi.org/10.1021/jp407397y | J. Phys. Chem. C 2013, 117, 22538–22544

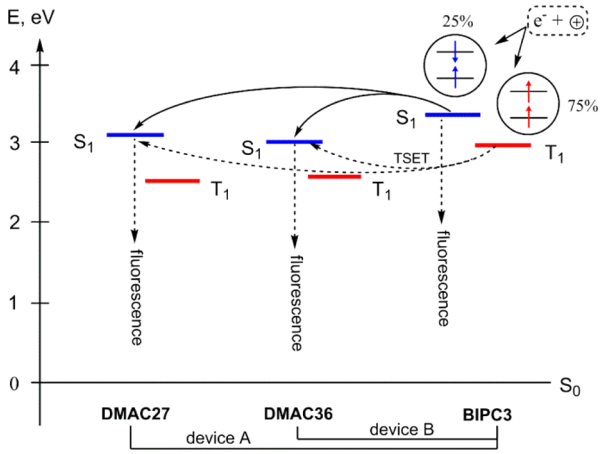

Figure 7. The calculated singlet and triplet energy levels of **DMAC27**, **DMAC36**, and **BIPC3** and the proposed scheme of electroluminescence in OLEDs A and B.

at 77 K.[24] In binary solvents, the decrease of the quantum yield and lifetime of the donor phosphorescence in the presence of the energy acceptor was observed simultaneously with the delayed fluorescence of acceptor at 77 K.[24,25] The inductive-resonance dipole–dipole mechanism of T–S energy transfer was proved in a number of studies.[24−27] The T–S energy transfer for **DMAC36** is much more effective than it is for **DMAC27**. The T_1 state energy of **BIPC3** (3 eV, Table 2) is in a perfect resonance with the S_1 level of **DMAC36** (3.05 eV). The S_1 energy level of **DMAC27** (3.13 eV) is far from the resonance, according to our TD DFT calculations (Table 2). This is in a good agreement with our observations and provides explanation of the 3-fold higher current efficiency and brightness of device B as compared with the corresponding characteristic of device A.

Figure 8 shows the current density–voltage characteristics and luminance–voltage characteristics of devices A and B. The turn-on voltage was found to be 3.4 V for both devices. Devices A and B exhibited high current efficiency values of 5.3 and 13.5 cd/A, respectively, and maximum brightness of 3 458 and 12 535 cd/m^2, respectively. These characteristics are comparable to those of the efficient electrophosphorescence devices.[4]

The energy difference between S_1 (**DMAC27**) and T_1 (**BIPC3**) prevents the effective resonance T_1–S_1 energy transfer in comparison with the almost degenerate S_1 (**DMAC36**) and T_1 (**BIPC3**) states. This fact explains the almost 3-fold higher measured external quantum efficiency of device B compared with that of device A. In addition, the fluorescence quantum yield of **DMAC27** in the condensed phase is much lower than that of **DMAC36**.[9]

Chromaticity coordinates (x, y) of devices A and B were found to be (0.19, 0.05) and (0.14, 0.06), respectively (Figure 9), which are very close to the National Television System Committee (NTSC) blue color standard of (0.14, 0.08).[28]

CONCLUSIONS

Highly efficient violet and blue organic electroluminescence devices were fabricated. They exhibit high current efficiency of 5.3 and 13.5 cd/A, high brightness of 3458 and 12535 cd/m^2 and high external quantum efficiency of 5 and 17%, respectively. We suggest that such high efficiency of the fabricated devices is due to efficient spin up-conversion from nonradiative triplet states of the host to radiative singlet states of the guests. To our knowledge, this is the first reported manifestation of triplet–singlet intermolecular energy transfer in OLEDs.

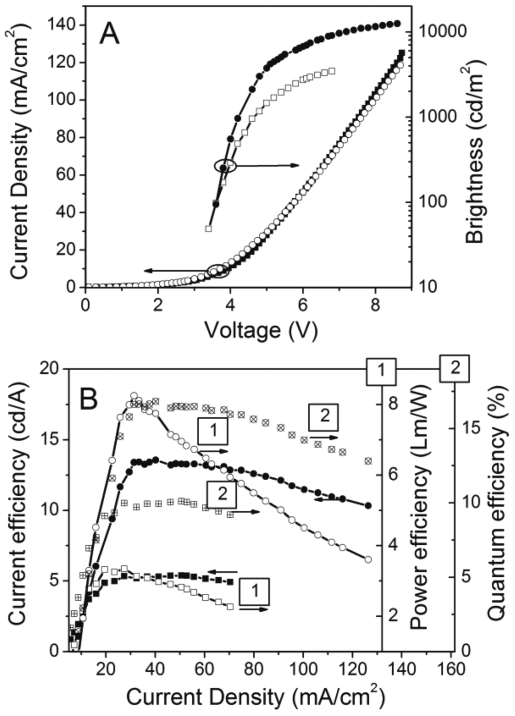

Figure 8. Current density–voltage and luminance–voltage characteristics for electroluminescent devices A (squares) and B (circles) (A) and current efficiency, quantum efficiency, and power efficiency–current density characteristics for devices A (squares) and B (circles) (B).

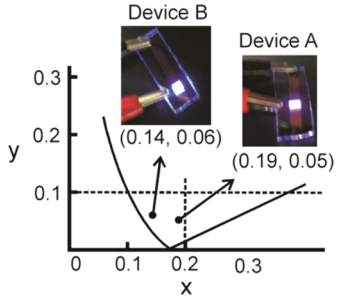

Figure 9. CIE 1931 chromaticity diagram and photos of devices A and B.

ASSOCIATED CONTENT

Supporting Information

Calculation of spin–orbit coupling matrix element in the host–guest complex (**BIPC3** and **DMAC36**). This material is available free of charge via the Internet at http://pubs.acs.org.

AUTHOR INFORMATION

Corresponding Author

*Department of Organic Technology, Kaunas University of Technology, Radvilenu pl. 19, LT-50254 Kaunas, Lithuania. Tel: +37037300193. E-mail: Juozas.Grazulevicius@ktu.lt.

Notes

The authors declare no competing financial interest.

■ ACKNOWLEDGMENTS

This research was supported by FP7 REGPOT-2012-2013-1 ICT Project CEOSeR (Grant Agreement 316010). It was also supported by the Lithuanian−Ukrainian Cooperation Program in the Fields of Research and Technologies (Project TAP LU 01/2012).

■ REFERENCES

(1) Wang, B.; Helander, M. G.; Qiu, J.; Puzzo, D. P.; Greiner, M. T.; Hudson, Z. M.; Wang, S.; Liu, Z. W.; Lu, Z. H. Unlocking the Full Potential of Organic Light-Emitting Diodes on Flexible Plastic. *Nat. Photonics* **2011**, *5*, 753−757.

(2) Shah, B. K; Neckers, D. C.; Shi, J.; Forsythe, E. W.; Morton, D. Photophysical Properties of Anthanthrene-Based Tunable Blue Emitters. *J. Phys. Chem. A.* **2005**, *109*, 7677−7681.

(3) Ma, Z.; Sonar, P.; Chen, Z.-K. Recent Progress in Fluorescent Blue Light-Emitting Materials. *Curr. Org. Chem.* **2010**, *14*, 2034−2069.

(4) Xiao, L.; Chen, Z.; Qu, B.; Luo, J.; Kong, S.; Gong, Q.; Kido, J. Recent Progresses on Materials for Electrophosphorescent Organic Light-Emitting Devices. *Adv. Mater.* **2011**, *23*, 926−952.

(5) Lee, J.-H.; Ho, Y.-H.; Lin, T.-C.; Wu, C.-F. High-Efficiency Fluorescent Blue Organic Light-Emitting Device with Balanced Carrier Transport. *J. Electrochem. Soc.* **2007**, *154*, J226−J228.

(6) Uoyama, H.; Goushi, K.; Shizu, K.; Nomura, H.; Adachi, C. Highly Efficient Organic Light-Emitting Diodes from Delayed Fluorescence. *Nature* **2012**, *492*, 234−238.

(7) Köhler, A.; Bässler, H. Triplet States in Organic Semiconductors. *Mater. Sci. Eng., R* **2009**, *66*, 71−109.

(8) Tsai, M. H.; Hong, Y. H.; Chang, C. H.; Su, H. C.; Wu, C. C.; Matoliukstyte, A.; Simokaitiene, J.; Grigalevicius, S.; Grazulevicius, J. V.; Hsu, C. P. 3-(9-Carbazolyl)carbazoles and 3,6-Di(9-carbazolyl)-carbazoles as Effective Host Materials for Efficient Blue Organic Electrophosphorescence. *Adv. Mater.* **2007**, *19*, 862−866.

(9) Tomkeviciene, A.; Puckyte, G.; Grazulevicius, J. V.; Kazlauskas, K.; Jursenas, S.; Jankauskas, V. Dimethyldiphenylamino-Substituted Carbazoles as Electronically Active Molecular Materials. *Dyes Pigm.* **2013**, *96*, 574−580.

(10) Keruckas, J.; Grazulevicius, J. V.; Volyniuk, D.; Cherpak, V.; Stakhira, P. 3,6-Bis(indol-1-yl)-9-phenylcarbazoles as Electroactive Materials for Electrophosphorescent Diodes. *Dyes Pigm.* **2014**, *100*, 66−72.

(11) Stakhira, P.; Cherpak, V.; Volynyuk, D.; Ivastchyshyn, F.; Hotra, Z.; Tataryn, V.; Luka, G. Characteristics of Organic Light Emitting Diodes with Copper Iodide as Injection Layer. *Thin Solid Films* **2010**, *518*, 7016−7018.

(12) Cherpak, V. V.; Stakhira, P. Y.; Volynyuk, D.Yu.; Simokaitiene, J.; Tomkeviciene, A.; Grazulevicius, J. V.; Bucinskas, A.; Yashchuk, V. M.; Kukhta, A. V.; Kukhta, I. N.; et al. 3,6-Di(9-carbazolyl)-9-(2-ethylhexyl)carbazole Based Single-Layer Blue Organic Light Emitting Diodes. *Synth. Met.* **2011**, *161*, 1343−1346.

(13) Stakhira, P.; Khomyak, S.; Cherpak, V.; Volyniuk, D.; Simokaitiene, J.; Tomkeviciene, A.; Kukhta, N. A.; Grazulevicius, J. V.; Kukhta, A. V.; Sun, X. W.; et al. Blue Organic Light-Emitting Diodes Based on Pyrazolinephenyl Derivative. *Synth. Met.* **2012**, *162*, 352−355.

(14) Tomkute-Luksiene, D.; Keruckas, J.; Malinauskas, T.; Simokaitiene, J.; Getautis, V.; Grazulevicius, J. V.; Volyniuk, D.; Cherpak, V.; Stakhira, P.; Yashchuk, V.; et al. 2-Phenyl-1,2,3-benzotriazole Ir(III) Complexes with Additional Donor Fragment for Single-Layer PhOLED Devices. *Dyes Pigm.* **2013**, *96*, 278−286.

(15) Greenham, N. C.; Friend, R. H.; Bradley, D. D. C. Measuring the Efficiency of Organic Light-Emitting Devices. *Adv. Mater.* **1994**, *6*, 491−494.

(16) Baldo, M. A.; Forrest, S. R.; Thompson, M. E. In *Organic Electroluminescence*; Kafafi, Z., Ed.; Taylor & Francis: New York, 2005.

(17) Becke, A. D. Density-Functional Exchange-Energy Approximation with Correct Asymptotic Behavior. *Phys. Rev. A* **1988**, *38*, 3098−3100.

(18) Lee, C.; Yang, W.; Parr, R. G. Development of the Colle-Salvetti Correlation-Energy Formula into a Functional of the Electron Density. *Phys. Rev. B* **1988**, *37*, 785−789.

(19) Francl, M. M.; Petro, W. J.; Hehre, W. J.; Binkley, J. S.; Gordon, M. S.; De Frees, D. J.; Pople, J. A. Self-Consistent Molecular Orbital Methods. XXIII. A Polarization Type Basis Set for Second-Row Elements. *J. Chem. Phys.* **1982**, *77*, 3654−3665.

(20) Frisch, M. J.; Trucks, G. W.; Schlegel, H. B.; Scuseria, G. E.; Robb, M. A.; Cheeseman, J. R.; Scalmani, G.; Barone, V.; Mennucci, B.; Petersson, G. A.; et al. *Gaussian 09*, Revision A.02; Gaussian Inc.: Wallingford, CT, 2009.

(21) Runge, E. Gross Density-Functional Theory for Time-Dependent Systems. *Phys. Rev. Lett.* **1984**, *52*, 997−1000.

(22) Miertus, S.; Scrocco, E.; Tomasi, J. Electrostatic Interaction of a Solute with a Continuum. A Direct Utilizaion of Ab Initio Molecular Potentials for the Prevision of Solvent Effects. *Chem. Phys.* **1981**, *55*, 117−129.

(23) Gorelsky, S. I. SWizard Program; http://www.sg-chem.net/; University of Ottawa: Ottawa, Canada, 2010.

(24) Ermolaev, V. L.; Sveshnikova, E. B. The Usage of Singlet-Triplet Transfer to the Study of the Internal Degradation of Electronic Energy in Organic Molecules. *Opt. Spectrosc.* **1964**, *16*, 588−593.

(25) Förster, T. The 10th Spiers Memorial Lecture. Transfer Mechanisms of Electronic Excitation. *Discuss. Faraday Soc.* **1959**, *27*, 7−17.

(26) Kellog, R. E.; Bennet, R. G. Radiationless Intermolecular Energy Transfer. III. Determination of Phosphorescence Efficiencies. *J. Chem. Phys.* **1964**, *41*, 3042−3045.

(27) Ermolaev, V. L.; Sveshnikova, E. B.; Bodunov, E. N. Inductive-Resonant Mechanism of Nonradiative Transitions in Ions and Molecules in Condensed Phase. *Phys.-Usp.* **1996**, *39*, 261−282.

(28) Tsai, T.-C.; Hung, W.-Y.; Chi, L.-C.; Wong, K.-T.; Hsieh, C.-C.; Chou, P.-T. A New Ambipolar Blue Emitter for NTSC Standard Blue Organic Light-Emitting Device. *Org. Electron.* **2009**, *10*, 158−162.